Water-Dispersible Porous Polyisoprene-*block*-Poly(acrylic acid) Microspheres

Zhihua Lu, Guojun Liu, Futian Liu

Department of Chemistry, University of Calgary, 2500 University Drive, NW, Calgary, Alberta, Canada T2N 1N4

ABSTRACT: Two polyisoprene-*block*-poly(*tert*-butyl acrylate) (PI-*b*-P*t*BA) samples and a poly(*tert*-butyl acrylate) (P*t*BA) homopolymer (hP*t*BA) were prepared by anionic polymerization and characterized by light scattering, size exclusion chromatography, and NMR. The *tert*-butyl groups were removed from one of the diblocks to yield amphiphilic polyisoprene-*block*-poly(acrylic acid) (PI-*b*-PAA). PI-*b*-PAA was then used as the surfactant to disperse dichloromethane containing PI-*b*-P*t*BA and hP*t*BA at different weight ratios as oil droplets in water. Solid microspheres containing segregated polyisoprene (PI) and P*t*BA/hP*t*BA domains were obtained after dichloromethane evaporation. Permanent microspheres were obtained after PI domain crosslinking with sulfur monochloride. Porous microspheres were produced after the hydrolysis of P*t*BA and the extraction of the homopoly(acrylic acid) chains. The shape and connectivity of the poly(acrylic acid)-lined pores were tuned by changes in the P*t*BA/hP*t*BA content in the precursor microspheres. © 2003 Wiley Periodicals, Inc. J Appl Polym Sci 90: 2785–2793, 2003

Key words: block copolymers; microgels; self-assembly; emulsion polymerization

INTRODUCTION

Microspheres are normally prepared by emulsion polymerization[1] and can also be prepared by precipitation polymerization.[2] Spheres with more complex architectures can be prepared by multistep sphere-seeded polymerization.[3–5] Pores are generated normally via the porogen-templating method, which involves porogen incorporation into microspheres during microsphere preparation and then its removal from the microspheres after microsphere preparation.[6] The porogen-templating method can be used to produce pores ranging in size from angstroms to micrometers by variations in the concentration and nature of the porogen, which can be a linear polymer, a solvent, or a nonsolvent for the microsphere matrix polymer. Under special conditions used for molecular imprinting,[7] one can also produce pores with a shape matching that of the templating porogen. This has, for example, been recently used to prepare diblock nanospheres with molecularly imprinted cores.[8] Pores can also be produced in microspheres containing poly(acrylic acid) (PAA) or poly(methacrylic acid) via the expansion of the polyelectrolyte chains upon their neutralization with a base.[9]

In general, pore size distributions prepared from the porogen-templating method are wide. It is also difficult to precisely control the size, shape, position, and density of pores produced inside each microsphere. Using an emulsion method that has been used extensively in the past to prepare microspheres from homopolymers,[10] we recently reported the preparation of microspheres with a uniform pore size and a controlled pore shape from a diblock precursor.[11] The synthesis involved dissolving the hydrophobic diblock poly(*tert*-butyl acrylate)-*block*-poly(2-cinnamoyloxyethyl methacrylate) (P*t*BA-*b*-PCEMA) in CH₂Cl₂ first. The oil phase was then sonicated in water containing a tailor-made diblock surfactant, poly(glyceryl methacrylate)-*block*-poly(2-cinnamoyloxyethyl methacrylate) (PGMA-*b*-PCEMA), the poly(glyceryl methacrylate) (PGMA) part being water-soluble, to make an emulsion. Microspheres containing segregated poly(*tert*-butyl acrylate) (P*t*BA) and poly(2-cinnamoyloxyethyl methacrylate) (PCEMA) domains were obtained after the evaporation of CH₂Cl₂. Permanent microspheres were prepared after the photocrosslinking of PCEMA. Microspheres with uniform and hexagonally packed PAA-lined nanochannels were obtained after *tert*-butyl group cleavage. The channels were then loaded with palladium nanoparticles to yield an efficient catalyst for alkene hydrogenation.[12]

Previous diblock microsphere preparation has resorted to PCEMA photocrosslinking, which is less cost-effective than chemical crosslinking. Reported in this article is the preparation of microspheres from polyisoprene-*block*-poly(*tert*-butyl acrylate) (PI-*b*-P*t*BA) and a P*t*BA homopolymer (hP*t*BA) with polyisoprene-*block*-poly(acrylic acid) (PI-*b*-PAA) as the surfactant:
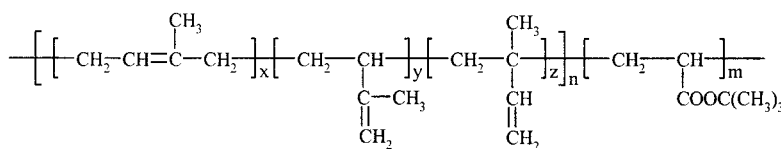
PI-*b*-P*t*BA

The polyisoprene (PI) domains of the microspheres are crosslinked, in this case by sulfur monochloride (S_2Cl_2). The pores are generated after the hydrolysis of the *tert*-butyl groups from P*t*BA/hP*t*BA and the extraction of the resultant PAA homopolymer (hPAA). Also reported is our ability to tune the shape of the P*t*BA/hP*t*BA domains inside the microspheres by the adjustment of the hP*t*BA content and thus the connectivity of the PAA-lined pores in the porous microspheres.

EXPERIMENTAL

Materials

Unless stated otherwise, all chemicals were purchased from Aldrich (Milwaukee, WI). Isoprene was distilled in the presence of *n*-butyl lithium, and *tert*-butyl acrylate (*t*BA) was purified by double distillation, first over CaH_2 and then in the presence of triethyl aluminum. Tetrahydrofuran (THF) was refluxed over potassium/benzophenone for at least 1 day and was distilled just before use. The phosphazene base *t*-BuP$_4$ ($C_{22}H_{63}N_{13}P_4$; Fluka; $1.00 \pm 0.02M$ in hexane) was purchased from Fluka (Ronkonkoma, NY), and used as received. Diphenyl ethylene (DPE) was distilled over CaH_2.

Polymer synthesis and characterization

Two PI-*b*-P*t*BA samples and hP*t*BA were synthesized by anionic polymerization. The polymerization was performed in a 1-L, three-necked, round-bottom flask. The flask was first flamed *in vacuo*. For the preparation of PI-*b*-P*t*BA, the procedure used by Förster and Krämer[13] for polyisoprene-*block*-poly(ethylene oxide) synthesis was modified and used. First added to the

flask was *t*-BuP$_4$ in hexane at a molar ratio of 1.05/1.00 relative to *sec*-butyl lithium (*s*-BuLi), which was to be added only later on. The solvent was evaporated, and the solid base was dried *in vacuo* overnight. After THF and isoprene transfer, the flask was cooled to −78°C, and *s*-BuLi was added. The polymerization was allowed to proceed for 5 h before DPE, at a 1.3 molar equivalence relative to *s*-BuLi, and LiCl, at a 3.0 molar equivalence to *s*-BuLi, were added to convert the PI anions into the sterically more hindered terminal DPE anions. The monomer *t*BA was polymerized for 3 h at −78°C before termination by methanol addition. After the evaporation of most of the THF, the polymer solution was added to ice crystals to precipitate out the polymer.

Equal molar amounts of DPE and *n*-BuLi were reacted to produce 1,1-diphenylhexyl lithium, which was used as the initiator for *t*BA homopolymerization at −78°C in THF. The resultant polymer was also purified by precipitation over ice crystals.

The polymers were characterized by ^{1}H-NMR, size exclusion chromatography (SEC), and light scattering (LS). SEC analysis was performed with a Styragel HT-4 broad-band column (Waters, Milford, MA) calibrated with poly(methyl methacrylate) standards. The eluent was THF. LS was done with a Brookhaven model 9025 instrument equipped with a 632.8-nm He–Ne laser (Holtsville, NY). The specific refractive-index increments (dn_r/dc) were determined for the diblocks at approximately 633 nm both in THF and in chloroform. The values in THF were 0.100 and 0.0734 mL/g for polymers 1 (with a higher PI content) and 2, respectively. The corresponding values in chloroform were 0.0543 and 0.0334 mL/g (Table I). The dn_r/dc value for hP*t*BA in methyl ethyl ketone (MEK) was 0.0808 mL/g.

TABLE I
Characteristics of the Polymers Used

Sample	dn_r/dc (mL/g)	Solvent for LS	LS M_w (g/mol)	M_w/M_n GPC	n/m NMR	n	m
1	0.0543	CHCl$_3$	9.2×10^4	1.22	5.0	980	200
1	0.100	THF	9.3×10^4				
2	0.0334	CHCl$_3$	6.6×10^4	1.23	0.50	200	410
2	0.0743	THF	6.7×10^4				
hP*t*BA	0.0808	MEK	1.40×10^4	1.24	—	—	110

TABLE II
Recipes and Properties for Different Batches of Microspheres

Batch	P1 (mg)	Surfactant (mg)	hP*t*BA (mg)	Sonication time (min)	PI conversion (%)	f_V (%)	DLS D_h (nm)	Fe^{3+} uptake capacity (mg/g)	Maximum $[Fe^{3+}]/[COOH]$
1	250	250	0	20	31	25	1900	8.5	0.079
2	50	25	0	60	30	25	240		
3	45	25	5	10	28	32	1650		
4	100	62.5	25	20	36	39	1870	35.0	0.335
5	35	25	15	10	29	47	1520		
6	90	75	60	20	33	54	1920	36.1	0.339

PI-*b*-PAA synthesis

The *tert*-butyl groups of polymer 2 were removed to yield PI-*b*-PAA according to a literature method.[14] This involved dissolving 4.3 g of the diblock in 20 mL of dichloromethane and 6 mL of trifluoroacetic acid. As the cleavage reaction progressed, 15 mL of dry THF was added gradually to improve the solubility of the intermediates. After 24 h, the mixture was concentrated by rotoevaporation and was then added dropwise into acetonitrile to precipitate PI-*b*-PAA. The polymer was further purified by the repetition of the routine of dissolution in THF and precipitation into acetonitrile. After drying, 2.2 g of the polymer was obtained in a 78% yield.

Microsphere preparation

Six batches of microspheres were prepared according to the recipes in Table II. For the preparation of batch 4 spheres, 62.5 mg of the diblock surfactant PI-*b*-PAA was dissolved in 0.5 mL of THF, and the solution was diluted to 25 mL by the gradual addition of water. The organic phase was prepared by the dissolution of polymer 1 (100 mg) and hP*t*BA (25 mg) in 2.5 mL of dichloromethane. The aqueous and organic solutions were then centrifuged at 2500 rpm or 1100*g* for the removal of any insoluble species, which were not visible but might have existed in negligible amounts, and the supernatants were mixed. After the mixture was ultrasonicated with a Branson 1200 sonicator, (Danbury, CT) for 20 min, the emulsion that formed was added over 45 min into 100 mL of water at 45°C and stirred at 300 rpm in an open, round-bottom flask. The mixture was stirred for another 1 h to further evaporate organic solvents and concentrated to approximately 20 mL by vacuum distillation. The mixture was then poured into a 14-cm petrifying dish, and 250 mg of cetyltrimethylammonium bromide (CTAB) was added. The dish was left in a fume hood to evaporate the residual water in open air in 2 days. After the powdery solid dried *in vacuo* for another 24 h, the particles were exposed to the vapor of S_2Cl_2 (36 mg; or at [C=C]/[S_2Cl_2] = 1.00/0.25) for 24 h to crosslink the

PI domains. The crosslinked microspheres were redispersed in water and separated from CTAB and excess diblock surfactant by centrifugation at 4000 rpm or 2750*g*. After drying, 115 mg of microspheres was produced.

Cleavage of *tert*-butyl groups

To cleave the *tert*-butyl groups from batch 4 spheres, the microspheres (100 mg) were dispersed in 20 mL of dichloromethane. Then added was 4 mL of trifluoroacetic acid. After the mixture was stirred at room temperature for 1 h, it was poured into 100 mL of methanol. The microspheres were separated from the solvent by centrifugation and redispersed in methanol. The microspheres were separated again by centrifugation after stirring in methanol for 24 h and were finally dried *in vacuo* for 12 h.

Scanning electron microscopy (SEM) and transmission electron microscopy (TEM)

For SEM, a microsphere powder was spread on a conductive carbon adhesive tape. The spheres were sputter-coated with an approximately 6-nm-thick Au–Pt layer and scanned with an FEI XL30 ESEM instrument operated at 20 kV (Hillsboro, OR). To obtain the internal structures of the microspheres with TEM, the microspheres (5 mg) were mixed with 0.05 mL of a 20 wt % polystyrene [Aldrich; weight-average molecular weight (M_w) = 20,000 g mol^{-1}, weight-average molecular weight/number-average molecular weight (M_w/M_n) = 5] solution in THF. The mixture was spread on a glass plate and dried in air overnight to obtain a film that was approximately 300 μm thick. The film was further dried at 70°C for 24 h and was sandwiched between two polystyrene plates, heated to 110°C, to an approximately 3-mm thickness for microtoming (Ultracut-E, Reichert-Jung, Vienna, Austria) into 40-nm-thick slices. The slices were picked up with Formvar-coated copper grids and stained with OsO_4 vapor for 12 h before being viewed under a

Hitachi H7000 (Tokyo, Japan) electron microscope operated at 75 kV.

Iron(III) uptake

A 20.0 ppm aqueous Fe^{3+} solution was prepared from $FeCl_3$. For kinetic studies, 10.0 mg of microspheres was stirred with 35.00 mL of the Fe^{3+} solution. At a predesignated time, the microspheres were separated from the supernatant by centrifugation at 2500 rpm for 0.5 min. The supernatant was further clarified by passage through a 0.45-μm Teflon filter. The residual Fe^{3+} concentration in the supernatant was analyzed according to a literature method.[15] It involved complex formation between Fe^{3+} and acetyl acetone and the quantification of the complex by UV–vis absorbance measurements at pH 3.5. The amount of Fe^{3+} that disappeared from the supernatant was equated to that sorbed by the spheres. For isotherms, the microspheres were stirred in Fe^{3+} solutions of different concentrations for at least 6 h before the solution was separated from the spheres for Fe^{3+} concentration analysis.

Dynamic light scattering (DLS) measurements

DLS was used to estimate the average size of the microspheres prepared. The instrument used was a Brookhaven 9025 model equipped with a 632.8-nm He–Ne laser. The crosslinked microspheres were dispersed at approximately 0.01 mg/mL in distilled water filtered through a 0.45-μm filter and used directly for LS measurements. The data were treated by the cumulant method.[16]

RESULTS AND DISCUSSION

Polymer characterization

Figure 1 shows the ^{1}H-NMR spectrum of polymer 2 in pyridine-d_5. The isoprene block contains three types of microstructures resulting from 1,2-, 3,4-, and 1,4-addition, and the contents of the structures were estimated by Förster and Krämer[13] from the intensity ratios of the vinyl proton peaks at 6.1, 5.0, and 5.3 ppm to be 28, 61, and 11%, respectively. Ratioing the peak intensity of the vinyl proton peaks between 5.0 and 6.1 ppm with that of PtBA at 1.45 ppm yielded $n/m = 0.50$ for this diblock. Polymer 1 has $n/m = 5.0$.

Similar M_w's were determined for the diblocks in both $CHCl_3$ and THF. The refractive index of PtBA should be approximately 1.46 according to the values for poly(n-butyl acrylate), poly(n-butyl methacrylate), and poly($tert$-butyl methacrylate).[17] This is very close to the refractive index of 1.446 for chloroform. On this basis, we reasoned that the PtBA block might be partially invisible in chloroform to the probing laser and
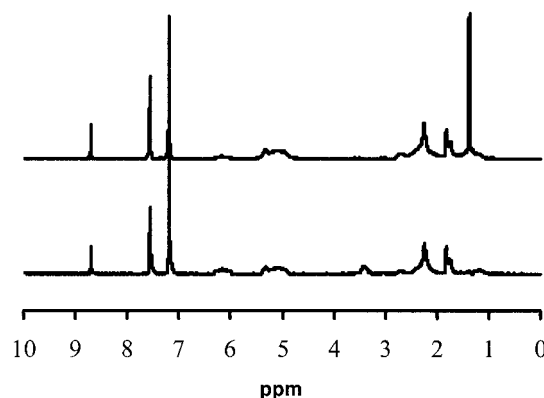

Figure 1   ^{1}H-NMR spectrum of polymer 2 in pyridine-d_5 (top). The vinyl protons for 1,2-, 3,4-, and 1,4-addition products are at 5.8, 4.7, and 4.9 ppm, respectively. The *tert*-butyl proton peak is at 1.45 ppm. Also shown for comparison is the NMR spectrum of polymer 2 after the removal of *tert*-butyl groups.

that the molar masses determined would be lower than the true values. This prompted us to recheck M_w in THF after the determination in chloroform as THF has a refractive index of 1.407. The superb agreement between M_w's determined in the two solvents suggests that our initial concern was an overreaction. Using M_w determined from LS and n/m from NMR, we found weight-average n and m values of 980 and 200 for polymer 1 and 200 and 410 for polymer 2, respectively. LS was also used to determine M_w for hPtBA, and the weight-average number of repeat units was 110. A relatively short hPtBA sample was used, mainly to ensure that the mixing between hPtBA and the PtBA block was effective and in the wet brush regime.[18]

In every case, the SEC polydispersity M_w/M_n was low at approximately 1.23. The true M_w/M_n values should be lower because we used only one broadband column with limited resolution for the characterization.

Figure 1 also shows the ^{1}H-NMR spectrum of polymer 2 after *tert*-butyl group removal. The quantitative removal of the *tert*-butyl groups is attested by the disappearance of the peak at 1.45 ppm. We also notice the emergence of a new peak at 3.4 ppm associated with the PAA carboxyl group protons.

Microsphere preparation

As mentioned in the Experimental section, the microsphere preparation involved first dispersing CH_2Cl_2 droplets containing PI-b-PtBA/hPtBA into water with the surfactant PI-b-PAA (Scheme 1). Dichloromethane evaporation at an elevated temperature, that is, 45°C, then led to solid polymer droplet formation. Because of the absence of strong interactions (hydrogen bonding, electrostatic interactions, etc.) between PI and PtBA, the two blocks were incompatible, and the mi-
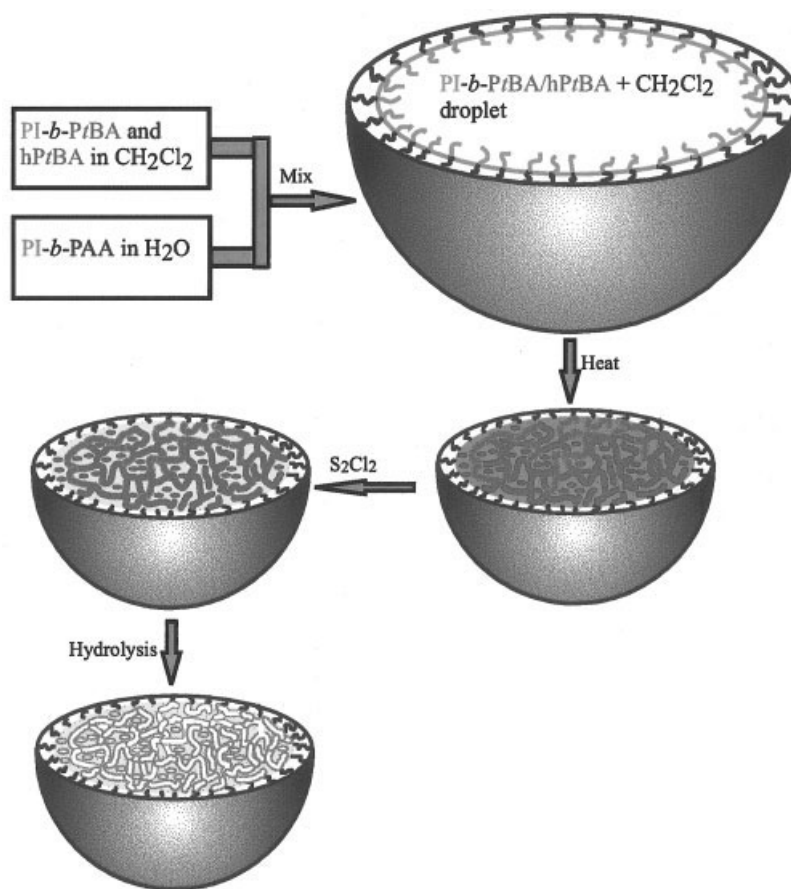
Scheme 1

nority P*t*BA block segregated from the majority PI block to yield nanometer-sized domains. As in the bulk solid, the exact morphology formed by P*t*BA/hP*t*BA varied with the volume fraction (f_V) in the polymer droplets or spheres. Scheme 1 depicts a wormlike morphology for the P*t*BA/hP*t*BA domains. The PI domains of the polymer spheres were crosslinked by S_2Cl_2. Nanospheres with PAA-lined channels were obtained after the hydrolysis of *tert*-butyl groups from the P*t*BA block and the extraction of the hPAA chains.

The protocol detailed in the Experimental section and depicted in Scheme 1 was reached after many optimization experiments. The experiments established that at a polymer-to-surfactant weight ratio of approximately 2, particles were produced with the narrowest size distribution. With the optimized protocol, six batches of microspheres were prepared with various P*t*BA/hP*t*BA f_V's (Table II). Figure 2 shows an SEM image of batch 4 spheres before *tert*-butyl group removal. Similar SEM images were obtained for other batches of spheres before and after *tert*-butyl group removal.

Although SEM images could be used to estimate the average size of the microspheres, a more accurate estimate was obtained from DLS. Plotted in Figure 3

are the hydrodynamic diameter (D_h) values of batch 1 and 4 spheres as a function of $\sin(\theta/2)$, where θ is the scattering angle. Extrapolating to a zero scattering angle yielded zero-angle hydrodynamic diameter (D_{h0}) values of 1900 and 1870 nm for the two samples. The D_{h0} values for the other samples were obtained in a similar fashion and are reported in Table II. Batch 1 and 2 spheres were prepared under exactly identical
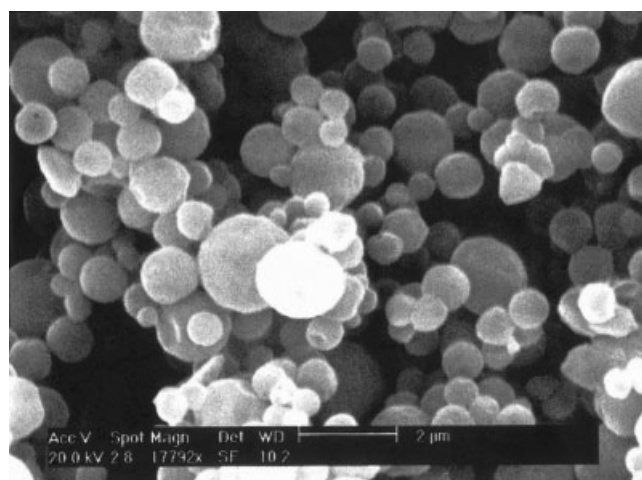
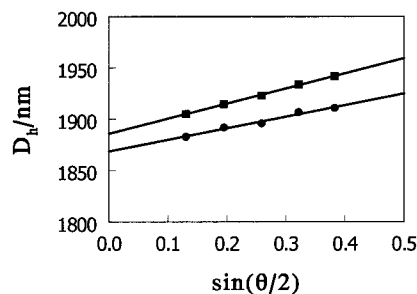**Figure 2** SEM image of batch 4 PI-*b*-P*t*BA microspheres.

Figure 3 Variation of D_h as a function of $\sin(\theta/2)$ for (■) batch 1 and (●) batch 4 spheres.

conditions, except for the sonication time. The D_{h0} results suggest that the microsphere size decreased with increasing ultrasonication time.

Chemical reactions

The porous microsphere preparation involved PI crosslinking by S_2Cl_2 and *tert*-butyl group removal. Because S_2Cl_2 reacts with water, we removed water in the presence of CTAB from the system before the microspheres were exposed to S_2Cl_2 vapor. CTAB, a cationic surfactant, was added to complex with the anionic PAA coronal chains.[19] Complex formation helped to prevent the direct contact and hydrogen-bond formation between different PAA chains and thus facilitated the production of a powdery solid and the easy redispersion of the microspheres in water.

The PI cylindrical domains were crosslinked via the reaction shown in Scheme 2.[20]

Figure 4(a) compares Fourier transform infrared (FTIR) spectra in the double-bond absorption region before and after batch 4 sphere treatment with S_2Cl_2. A quantitative analysis of the double-bond absorption decrease at 1640 cm^{-1} after the reaction gave a double-bond conversion of 36%. This is lower than but close to 50%, which is expected from the isoprene-to-S_2Cl_2 molar ratio used in the reaction. A lower conversion can be partially explained by the presence of trace amounts of impurities such as water in the system. Also, the PAA groups might react with S_2Cl_2 as well.

The *tert*-butyl groups in the P*t*BA/hP*t*BA domains were cleaved by a treatment with CF_3COOH in dry CH_2Cl_2. The effectiveness of this treatment is demon-
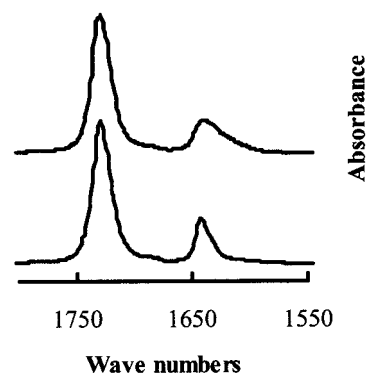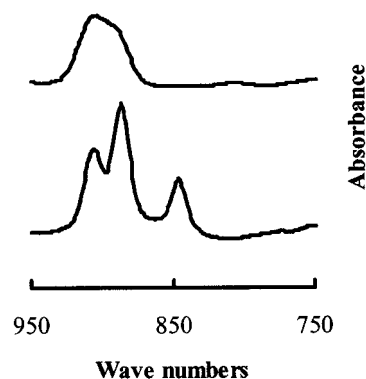

Figure 4 (a) Spectra for batch 4 microspheres in the double-bond absorption region (1640 cm^{-1}) before (bottom) and after (top) treatment with S_2Cl_2 and (b) spectra for batch 4 microspheres in the *t*-butyl ester absorption region (846 cm^{-1}) before (bottom) and after (top) treatment with CF_3COOH.

strated by the FTIR results in Figure 4(b). After the treatment, the rocking band of the *tert*-butyl groups at 846 cm^{-1} disappeared completely.[21]

Internal morphologies of the spheres

Figure 5(a–c) shows TEM images of thin sections of batch 1, 4, and 6 spheres after PI crosslinking. The thin sections were stained with OsO_4, and so the P*t*BA domains appear light. P*t*BA forms a mixture of spheres and cylinders in the crosslinked PI matrix for batch 1 spheres. A wormlike morphology is found for
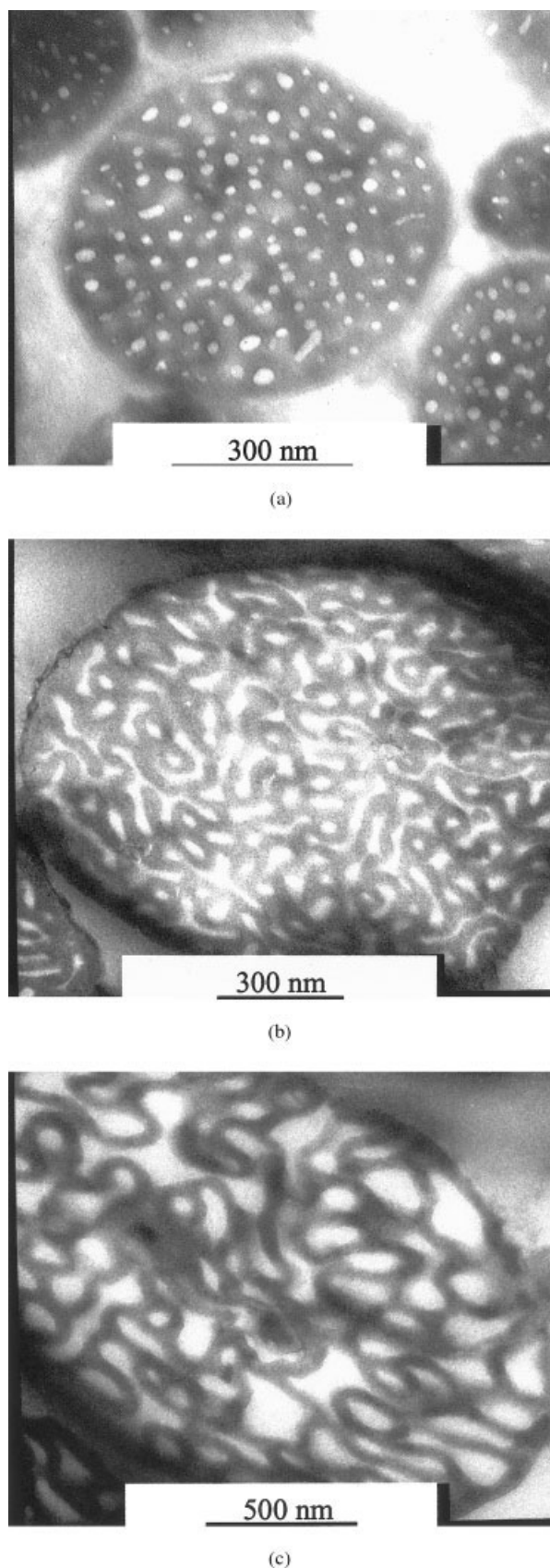

Scheme 2

(a)

(b)

(c)
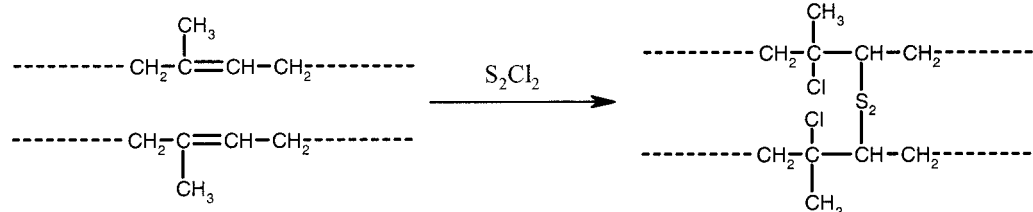
Figure 5 TEM images of thin sections of (a) batch 1, (b) batch 4, and (c) batch 6 microspheres. The samples were stained with OsO$_4$.

P*t*BA/hP*t*BA domains in batch 4 spheres. The P*t*BA domain size in batch 6 spheres increases with respect to that found in batch 4 spheres. It is, however, difficult to define the morphology of such domains, as they are irregularly shaped.

We demonstrated previously[11–12] for another system that the surfactant utilization or incorporation efficiency was low. Thus, the final sphere composition is approximately determined by the PI-*b*-P*t*BA and hP*t*BA contents. We previously reported a density of 1.02 g/mL for P*t*BA,[22] and the density of PI was reported by Hashimoto et al.[23] to be 0.92 g/mL. Using these density values and the polymer feed weight ratios, we calculated the P*t*BA f_V for each sample with the data shown in Table II. The P*t*BA/hP*t*BA f_V's for batch 1, 4, and 6 spheres were 25, 39, and 54%, respectively.

In bulk, we expect the equilibrium morphology for the minor block of a diblock to change from spheres to cylinders, gyroids or hexagonally perforated layers (HPLs), and lamellae as its f_V increases from approximately 20 to approximately 30, 38, and 50%, respectively.[24] A gyroid is formed at $f_V \approx 0.38$ if the two blocks are moderately incompatible, and HPLs are obtained if the two blocks are strongly incompatible. The fact that P*t*BA at $f_V \approx 0.25$ formed a mixture of spheres and cylinders in microspheres suggests the applicability of the bulk phase rule in the confined space of the microspheres as well. The wormlike morphology found in batch 4 spheres can also be loosely related to the gyroid morphology found in bulk. We can, however, hardly relate the morphology found in batch 6 spheres to the bulk lamellar morphology. In batch 6 spheres, the hP*t*BA weight ratio relative to PI-*b*-P*t*BA reached 67%. At such a high homopolymer content, homopolymers have been previously seen to undergo macrophase separation.[18] The macrophase-separated domains may not have regular sizes and shapes.

Porous spheres

Figure 6(a,b) shows TEM images of batch 3 and 6 spheres after *t*-butyl group removal. Such images were obtained without the use of chemical staining, and the contrast was derived from the polymer density difference. The fact that the original P*t*BA domains now look light suggests *tert*-butyl group removal and the extraction of hPAA. The extraction of hPAA can also be deduced from a close examination of Figure 6(b). Although the P*t*BA domains in Figure 5(c) look uniformly light, the corresponding regions in Figure 6(b) have various shades. Those locations that are the lightest probably correspond to voids left behind from hPAA extraction.

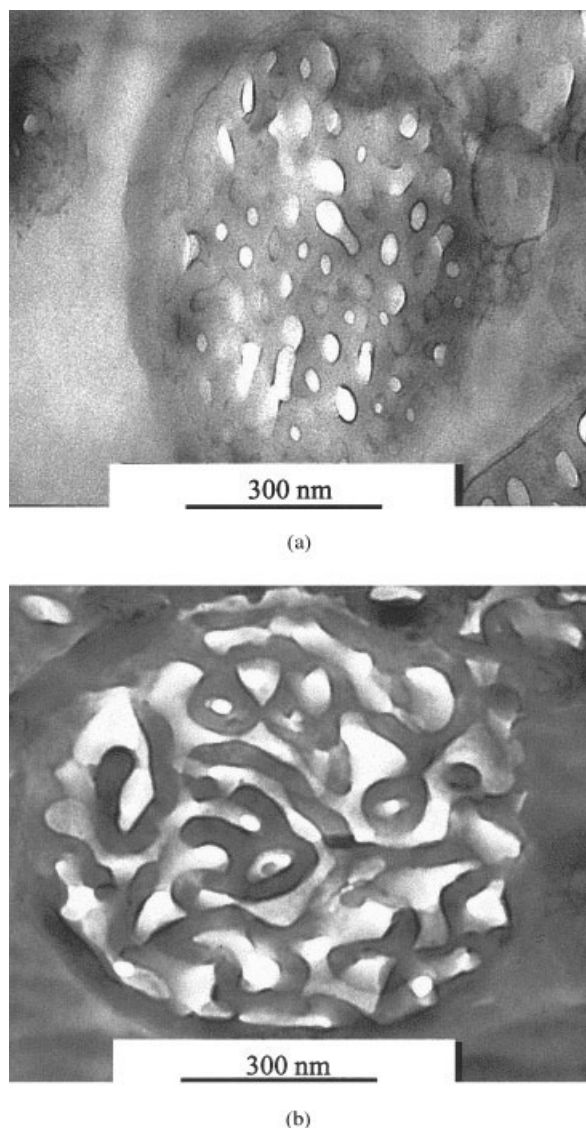We performed gravimetric and NMR analyses of products extracted from hydrolyzed batch 4 and 6

(a)

(b)

Figure 6 TEM images of thin sections of (a) batch 3 and (b) batch 6 microspheres after *tert*-butyl cleavage. The samples were not stained.

spheres. hPAA was indeed removed quantitatively from the spheres with our protocol, as described in the Experimental section. Thus, we have indeed produced PI-*b*-PAA microspheres with PAA-lined nanochannels.

Properties of the microspheres

The microspheres were dispersible in water, and the internal PAA domains were able to bind cations such as Cu^{2+} and Fe^{3+}. Figures 7 and 8 show the kinetic and isothermal data of the Fe^{3+} uptake by batch 1, 4, and 6 microspheres. Because the microspheres were added as solids and the dispersion of the microspheres in the Fe^{3+} solution might be rate-limiting, a quantitative treatment of the uptake kinetic data was meaningless. The qualitative feature that emerged
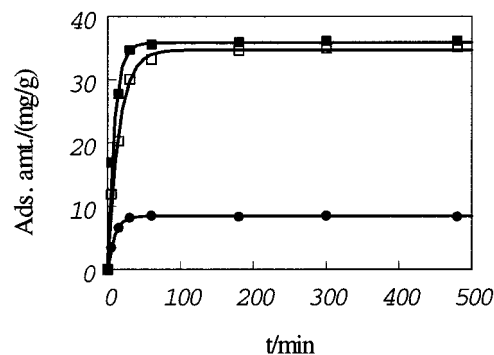

Figure 7 Kinetic data of Fe^{3+} uptake by (●) batch 1, (□) batch 4, and (■) batch 6 microspheres.

from the data was that Fe^{3+} sorption equilibrium was established fast (e.g., in ca. 50 min) in each case. The isothermal data are also plotted in Figure 8 in terms of the molar ratio ($[Fe^{3+}]/[COOH]$) between bound Fe^{3+} and the available carboxyl groups in each gram of microspheres. In the calculations, we assumed that hPAA was fully extracted out of the spheres, an assumption valid only for batch 4 and 6 spheres but not for batch 1 spheres. We further assumed that each S_2Cl_2 reacted with 2 mol of double bonds. The fact that the maximum $[Fe^{3+}]/[COOH]$ value reached the theoretical binding stoichiometry of batches 4 and 6 suggests the full accessibility of the carboxyl groups in these cases. Thus, the different degrees of carboxyl group accessibility between batch 1 spheres and batch 4 and 6 spheres reconfirmed the results of the morphological studies.

CONCLUSIONS

Two PI-*b*-P*t*BA samples and an hP*t*BA sample were prepared by anionic polymerization and characterized by LS, SEC, and NMR. The *tert*-butyl groups were removed from one of the samples to yield an amphiphilic diblock copolymer, PI-*b*-PAA. PI-*b*-P*t*BA and hP*t*BA at different weight ratios were then dissolved
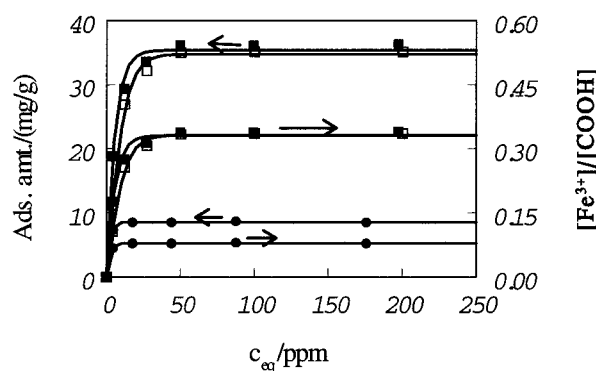

Figure 8 Isothermal data of Fe^{3+} uptake by (●) batch 1, (□) batch 4, and (■) batch 6 microspheres.

in dichloromethane and dispersed in water as oil droplets with PI-*b*-PAA as the surfactant. Solid microspheres were obtained after the evaporation of dichloromethane. The PI and P*t*BA polymers were segregated in the microspheres. The P*t*BA/hP*t*BA domain shape changed from spheres and cylinders to a continuous wormlike phase as the hP*t*BA content increased. Permanent microspheres were obtained after the crosslinking of the PI domains by S_2Cl_2. Porous microspheres were produced after the hydrolysis of P*t*BA and the extraction of the hPAA chains. All of the carboxyl groups in the microspheres containing a continuous wormlike P*t*BA/hP*t*BA phase after P*t*BA hydrolysis participated in Fe^{3+} binding. The bound cations could be further derivatized[21,25] to yield water-dispersible magnetic microspheres with potential applications in diagnostics.

References

1. Gan, L. M.; Chew, C. H. Polymer Materials Encyclopedia; CRC: Boca Raton, FL, 1996; p 4321.
2. Li, W. H.; Stöver, H. D. H. J Polym Sci Part A: Polym Chem 1998, 36, 1543.
3. Bradford, E. B.; Vanderhoff, J. W. J Appl Phys 1955, 26, 684.
4. Ugelstad, J.; Kaggerud, K. H.; Hansen, F. K.; Berger, A. Makromol Chem 1979, 180, 737.
5. Wang, Q. C.; Švec, F.; Fréchet, M. J. J Polym Sci Part A: Polym Chem 1994, 32, 2577.
6. (a) Seidl, J.; Malinsky, J.; Dusek, K.; Heitz, W. Adv Polym Sci 1967, 5, 113; (b) Guyot, A.; Bartholin, M. Prog Polym Sci 1982, 8, 277.
7. (a) Wulff, G. Angew Chem Int Ed 1995, 34, 1812; (b) Steinke, J.; Sherrington, D. C.; Dunkin, I. R. Adv Polym Sci 1995, 123, 81; (c) Shea, K. J. Trends Polym Sci 1994, 2, 166; (d) Sellergren, B. Angew Chem Int Ed 2000, 39, 1032.
8. (a) Zhou, J. Y.; Li, Z.; Liu, G. J. Macromolecules 2002, 35, 3690; (b) Liu, G. J.; Zhou, J. Y. Macromolecules 2002, 35, 8167; (c) Lin, G. J.; Zhou, J. Y. Macromolecules 2003, 36, 876.
9. Okubo, M. Polymer Materials Encyclopedia; CRC: Boca Raton, FL, 1996; p 4537.
10. Nakache, E.; Poulain, N.; Candau, F.; Orecchioni, A.-M.; Irache, J. M. In Handbook of Nanostructured Materials and Nanotechnology; Nalwa, H. S., Ed.; Academic: San Diego, 2000; Vol. 5, p 577; see also references therein.
11. Lu, Z.; Liu, G.; Liu, F. Macromolecules 2001, 34, 8814.
12. Lu, Z.; Liu, G.; Phillips, H.; Hill, J. M.; Chang, J.; Kydd, R. A. Nano Lett 2001, 1, 683.
13. Förster, S.; Krämer, E. Macromolecules 1999, 32, 2783.
14. (a) Bryan, D. B.; Hall, R. F.; Holden, K. G.; Huffman, W. F.; Gleanson, J. G. J Am Chem Soc 1977, 99, 2353; (b) Greene, T. W.; Wuts, P. G. M. Protective Groups in Organic Synthesis, 3rd ed.; Wiley: New York, 1999; (c) Ma, Q. G.; Wooley, K. L. J Polym Sci Part A: Polym Chem 2000, 38, 4805; (d) Li, Z.; Liu, G. J.; Law, S.-J.; Sells, T. Biomacromolecules, to appear.
15. (a) Pulsifer, H. B. J Am Chem Soc 1904, 26, 967; (b) Wenger, P.; Duchert, R. Helv Chim Acta 1944, 27, 757.
16. Berne, B. J.; Pecora, R. Dynamic Light Scattering with Applications to Chemistry, Biology, and Physics; Dover: Mineola, NY, 2000.
17. Brandrup, J.; Immergut, E. H. Polymer Handbook, 3rd ed.; Wiley: New York, 1989.
18. Hesagawa, H.; Hashimoto, T. Comprehensive Polymer Science; Pergamon: London, 1996.
19. Kabanov, A. V.; Bronich, T. K.; Kabanov, V. A.; Yu, K.; Eisenberg, A. J Am Chem Soc 1998, 120, 9941.
20. Ishizu, K.; Onen, A. J Polym Sci Part A: Polym Chem 1989, 27, 3721.
21. Underhill, R. S.; Liu, G. J. Chem Mater 2000, 12, 2082.
22. Liu, G. J.; Ding, J. F.; Hashimoto, T.; Saijo, K.; Winnik, F. M.; Nigam, S. Chem Mater 1999, 11, 2233.
23. Inoue, T.; Soen, T.; Hashimoto, T.; Kawa, H. J Polym Sci Part A-2: Polym Chem 1969, 7, 1283.
24. Bates, F. S.; Fredrickson, G. H. Phys Today 1999, February, 32.
25. Yan, X. H.; Liu, G. J.; Liu, F. T. Angew Chem Int Ed 2001, 40, 3593.